

12. C. J. Roberts *et al.*, *Science* **287**, 873 (2000).
13. Fus3 is known to autophosphorylate and autoactivate (7), as is the Erk2 MAPK (28).
14. J. Bardwell, L. J. Flatauer, K. Matsukuma, J. Thorner, L. Bardwell, *J. Biol. Chem.* **276**, 10374 (2001).
15. Single-letter abbreviations for the amino acid residues are as follows: A, Ala; C, Cys; D, Asp; E, Glu; F, Phe; G, Gly; H, His; I, Ile; K, Lys; L, Leu; M, Met; N, Asn; P, Pro; Q, Gln; R, Arg; S, Ser; T, Thr; V, Val; W, Trp; and Y, Tyr.
16. M. J. Cismowski, M. V. Metodiev, E. M. Draper, D. E. Stone, *Biochem. Biophys. Res. Commun.* **284**, 247 (2001).
17. The halos formed by *gpa1<sup>K21E R22E</sup>* cells were reproducibly 2 mm larger than those formed by wild-type cells.
18. K. Madura, A. Varshavsky, *Science* **265**, 1454 (1994).
19. K. Bence, W. Ma, T. Kozasa, X. Y. Huang, *Nature* **389**, 296 (1997).
20. Y. Jiang *et al.*, *Nature* **395**, 808 (1998).
21. Y.-C. Ma, J. Huang, S. Ali, W. Lowry, X.-Y. Huang, *Cell* **102**, 635 (2000).
22. C. S. Shi, S. Sinnarajah, H. Cho, T. Kozasa, J. H. Kehrl, *J. Biol. Chem.* **275**, 24470 (2000).
23. R. Dorer, P. M. Pryciak, L. H. Hartwell, *J. Cell Biol.* **131**, 854 (1995).
24. H.-A. Fujimura, *J. Cell Sci.* **107**, 2617 (1994).
25. E. Li, M. J. Cismowski, D. E. Stone, *Mol. Gen. Genet.* **258**, 608 (1998).
26. G. M. Cole, S. I. Reed, *Cell* **64**, 703 (1991).
27. S. Offermanns, V. Mancino, J.-P. Revel, M. I. Simon, *Science* **275**, 533 (1997).
28. F. A. Gonzalez, D. L. Raden, M. Rigby, R. J. Davis, *FEBS Lett.* **304**, 170 (1992).
29. We thank S. Reed and L. Hartwell for plasmids, A. Ellicott and H.-j. Kim for technical assistance, S. Zaichick for the photomicrographs, and Nava Segev and Holly Stratton for critical reading of the manuscript. Supported by grants from the American Cancer Society and NSF (D.E.S.)

**Supporting Online Material**  
[www.sciencemag.org/cgi/content/full/296/5572/1483/DC1](http://www.sciencemag.org/cgi/content/full/296/5572/1483/DC1)

Materials and Methods  
 Figs. S1 to S4

4 February 2002; accepted 5 April 2002

# Induction of Cachexia in Mice by Systemically Administered Myostatin

Teresa A. Zimmers,<sup>1\*</sup> Monique V. Davies,<sup>2</sup>  
 Leonidas G. Koniaris,<sup>1\*</sup> Paul Haynes,<sup>2†</sup> Aurora F. Esqueda,<sup>1</sup>  
 Kathy N. Tomkinson,<sup>2</sup> Alexandra C. McPherron,<sup>1</sup>  
 Neil M. Wolfman,<sup>2</sup> Se-jin Lee<sup>1‡</sup>

Mice and cattle with genetic deficiencies in myostatin exhibit dramatic increases in skeletal muscle mass, suggesting that myostatin normally suppresses muscle growth. Whether this increased muscling results from prenatal or postnatal lack of myostatin activity is unknown. Here we show that myostatin circulates in the blood of adult mice in a latent form that can be activated by acid treatment. Systemic overexpression of myostatin in adult mice was found to induce profound muscle and fat loss analogous to that seen in human cachexia syndromes. These data indicate that myostatin acts systemically in adult animals and may be a useful pharmacologic target in clinical settings such as cachexia, where muscle growth is desired.

Myostatin [growth/differentiation factor-8 (GDF-8)] is a transforming growth factor- $\beta$  (TGF- $\beta$ ) family member that is essential for proper regulation of skeletal muscle mass (1). Myostatin is expressed almost exclusively in cells of the skeletal muscle lineage, from embryonic myotome to striated muscle in adults. Mice carrying a targeted deletion of the gene encoding myostatin (*Mstn*<sup>-/-</sup>) have a dramatic and widespread increase in muscle mass, suggesting that myostatin normally acts as a negative regulator of muscle growth. Individual muscles of *Mstn*<sup>-/-</sup> mice weigh ~100 to 200% more than those of control animals as a result of muscle fiber hypertrophy and hyperplasia. Although myostatin

does not appear to be essential for either viability or fertility, *Mstn* has been remarkably well conserved through evolution; hu-

man, rat, murine, porcine, turkey, and chicken myostatin protein sequences are identical in the biologically active COOH terminus of the protein (2). The function of myostatin also appears to have been conserved, as *Mstn* mutations in cattle cause the double-muscling phenotype (2–5). Because the myostatin loss-of-function phenotype could result entirely from lack of myostatin activity during embryonic development, the role that myostatin plays in adult animals is unknown.

To determine whether myostatin acts in an endocrine fashion in adult mice, we sought to identify myostatin in serum. Myostatin is synthesized as a pre-proprotein activated by two proteolytic cleavages. Removal of the signal sequence is followed by cleavage at a tetrabasic processing site, resulting in a 26-kD NH<sub>2</sub>-terminal propeptide and a 12.5-kD COOH-terminal peptide, a dimer of which is the biologically active portion of the protein. Western blot analysis revealed a 12.5-kD protein in the serum of wild-type but not *Mstn*<sup>-/-</sup> mice that comigrated with purified recombinant myostatin (Fig. 1A).

Next, we measured myostatin activity in

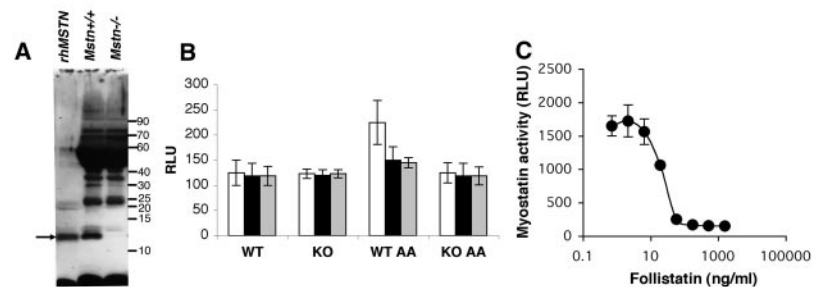


**Fig. 1.** Detection of myostatin protein and activity. (A) Recombinant myostatin (rhMSTN) and serum samples (5  $\mu$ l) from wild-type (*Mstn*<sup>+/+</sup>) and *Mstn*<sup>-/-</sup> mice were subjected to SDS-polyacrylamide gel electrophoresis (SDS-PAGE) under reducing conditions. Western blot analysis was then performed with the use of a rabbit polyclonal antiserum raised against bacterially expressed recombinant myostatin COOH-terminal protein. Location of myostatin COOH-terminal monomer is indicated by arrow. Higher molecular weight bands were also detected in the serum of both wild-type and knockout mice, including a clear band around 25,000. Similar nonspecific bands may have given rise to the identification in other reports of a 26-kD "myostatin-related protein" in the blood (27) and muscle (27–31) of mice and humans. (B) A204 assay (6) of serum myostatin activity in normal and acid-activated (AA) wild-type (WT) and *Mstn*<sup>-/-</sup> (KO) serum samples, in the presence of no added factor (white bars), 500 ng/ml propeptide (black bars), or 500 ng/ml follistatin (gray bars). Such data, in comparison to standard curves generated with recombinant myostatin diluted in serum (fig. S1; see Materials and Methods in SOM), led us to estimate the concentration of mouse serum myostatin to be around 80 ng/ml. (C) Inhibition of 5 ng/ml recombinant COOH-terminal myostatin in the A204 assay by preincubation with follistatin. RLU, relative luciferase units. Error bars are  $\pm$  SD.

<sup>1</sup>Department of Molecular Biology and Genetics, Johns Hopkins School of Medicine, 725 North Wolfe Street, Baltimore, MD 21205, USA. <sup>2</sup>Wyeth Research Division, Wyeth Pharmaceuticals, Inc., 87 CambridgePark Drive, Cambridge, MA 02140, USA.

\*Present address: Department of Surgery, University of Rochester School of Medicine and Dentistry, 601 Elmwood Avenue, Box SURG, Rochester, NY 14642, USA.

†Present address: Torrey Mesa Research Institute, 3115 Merryfield Row, San Diego, CA 92121, USA.

‡To whom correspondence should be addressed. E-mail: sjlee@jhmi.edu

## REPORTS

serum samples with the use of the pGL3-(CAGA)<sub>12</sub> luciferase reporter assay (fig. S1) (6) but noted no difference in luciferase activity with wild-type serum versus *Mstn*<sup>-/-</sup> serum (sensitivity, ~20 ng/ml myostatin) (Fig. 1B). One potential explanation for this result is that serum myostatin may be held in an inactive or latent complex with its propeptide, as has been described for TGF- $\beta$  (7–11). Dissociation of the latent complex by treatment with acid releases mature TGF- $\beta$  for binding to its receptors (12, 13). Similarly, acid treatment of wild-type serum resulted in a twofold increase in luciferase activity over background levels, whereas no increase in activity was detected in acid-treated serum samples from *Mstn*<sup>-/-</sup> mice (Fig. 1B). Furthermore, the myostatin activity in acid-activated wild-type serum was neutralized by the addition of either recombinant myostatin propeptide or follistatin, both of which are known to inhibit myostatin biological activity in vitro and in vivo (Fig. 1C) (6, 14). Therefore, like TGF- $\beta$  and the activins, myostatin

may be regulated in vivo by the association and dissociation of binding proteins, including perhaps propeptide and follistatin or related molecules (15).

To investigate whether myostatin acts systemically, we delivered high levels of circulating myostatin by injecting into the thighs of athymic nude mice a Chinese hamster ovary (CHO) cell line that produces murine myostatin under control of a zinc-inducible metallothionein promoter (1, 14) [see Materials and Methods in supporting online material (SOM)]. Sixteen days after injection, mice bearing control tumors (CHO-control) appeared healthy, whereas CHO-myostatin tumor-bearing mice were dramatically wasted with a hunchback and sunken-eye appearance. Strikingly, all CHO-control mice had gained or maintained body mass, whereas CHO-myostatin mice had lost, on average, 33% of total body weight (Fig. 2, A and B). Part of this weight loss was due to a global decline in skeletal muscle mass, as examination of individual muscles distant from the injection site revealed declines of 35 to 50%

(Fig. 2, C and D). A near-total loss of white adipose tissue also contributed to weight loss (Fig. 2, E and F). This muscle and fat wasting was accompanied by significant declines in tail blood glucose, with CHO-myostatin mice exhibiting severe hypoglycemia by day 16 (Fig. 2G).

Four lines of evidence suggested that myostatin production from the injected CHO cells caused the wasting syndrome. First, individual injections of 10 other CHO-cell lines expressing other proteins resulted in tumor growth but no weight loss (16) (see Materials and Methods in SOM). Second, providing mice with water containing zinc sulfate as opposed to tap water accelerated weight loss in CHO-myostatin mice (fig. S2; see Materials and Methods in SOM), consistent with heavy metal-enhanced expression of myostatin from the metallothionein promoter (16). Third, we observed increased serum myostatin activity with increased weight loss (Fig. 2H). Fourth, twice-daily injections of 1- $\mu$ g myostatin COOH-terminal dimer resulted in a ~50% reduction (versus carrier) in white fat in the intrascapular ( $0.199 \pm 0.064$  g versus  $0.436 \pm 0.053$  g,  $P = 0.002$ ), periuterine ( $0.047 \pm 0.022$  g versus  $0.111 \pm 0.026$

**Fig. 2.** Analysis of mice injected with CHO-myostatin cells or with a similarly selected cell line expressing no recombinant protein (CHO-control). Error bars are  $\pm$  SE. (A to G) Time course of wasting syndrome in CHO-myostatin mice (open squares) compared with CHO-control mice (solid circles). \* $P < 0.01$ ; \*\* $P < 0.001$ .  $n = 6$  to 24 mice per point. (A) Tumor mass. As expected, both cell lines produced localized tumors with no evidence of metastasis. (B) Total body weight (symbols as above), tumor-free body weight in CHO-control (open circles) and CHO-myostatin mice (solid squares). CHO-myostatin mouse weight loss was not due to dehydration, as carcass water content did not differ between groups ( $65.3\% \pm 0.6\%$  versus  $65.5\% \pm 1.8\%$ ). (C and D) Weights of gastrocnemius and pectoralis muscles, respectively, from tumor-free sides. Quadriceps, tibialis anterior, and triceps femoris weights were also reduced 35, 37, and 45%, respectively, in CHO-myostatin mice at day 16 (16). (E and F) Weights of periuterine fat pad and retroperitoneal fat pads, respectively, from tumor-free sides. Inguinal and intrascapular white fat pad weights were also reduced 96 to 99% in CHO-myostatin mice at day 16 (16). Similarly, substantial reductions in carcass fat (~38%) were measured in CHO-myostatin mice at day 16 ( $16.8\% \pm 2.0\%$  versus  $27.1\% \pm 2.4\%$ ,  $P = 0.006$ ) (see Materials and Methods in SOM). (G) Tail blood glucose measurement demonstrates progressive hypoglycemia in CHO-myostatin mice. (H) Unactivated (gray bars) and acid-activated (black bars) myostatin activity in serum of CHO-myostatin mice. Even untreated sera from CHO-myostatin mice showed activity in the reporter gene assay, suggesting that very high levels of myostatin may dysregulate the mechanisms controlling latency and activation. (I) Food consumed per CHO-myostatin (black bars) or CHO-control (white bars) mouse per day for the indicated time intervals after injection. Differences were not significant.

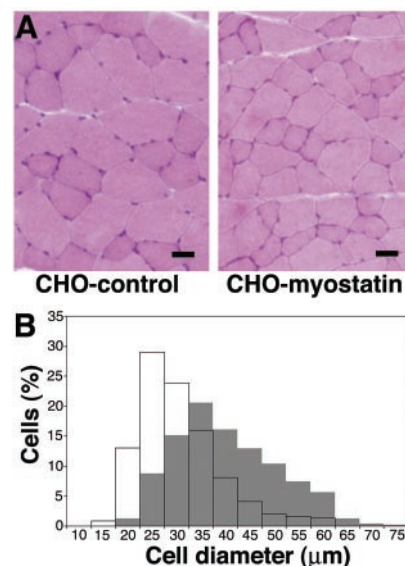
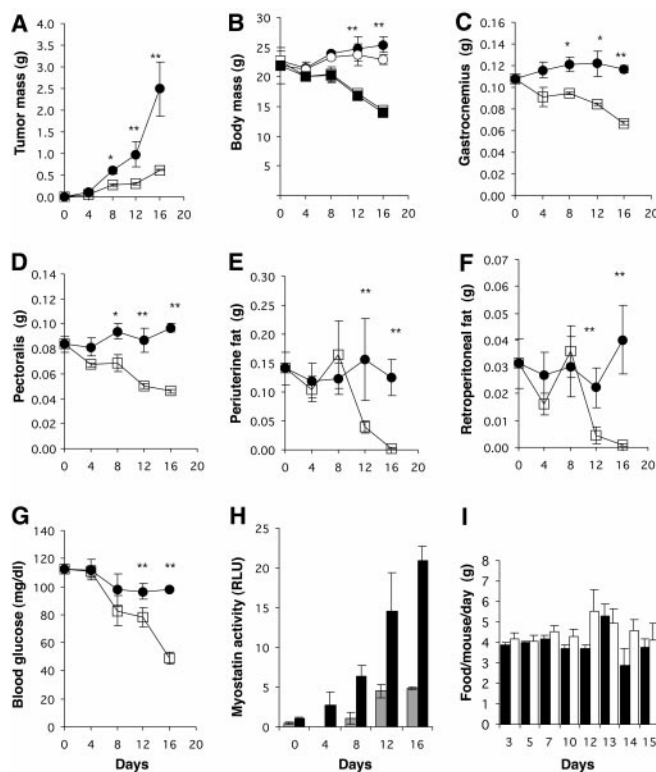


**Fig. 3.** Effects of myostatin overexpression on skeletal muscle. (A) Hematoxylin and eosin-stained, frozen gastrocnemius cross sections from non-tumor bearing limbs of CHO-control and CHO-myostatin mice at day 16. Bar, 25  $\mu$ m. (B) Muscle fiber size distribution in gastrocnemius of CHO-control (shaded bars,  $n = 948$ ) and CHO-myostatin (open bars,  $n = 438$ ) mice at day 16 determined as described (7). Mean CHO-myostatin fiber diameter was reduced by 25% compared with CHO-control ( $28.4 \pm 8.4$   $\mu$ m versus  $38.2 \pm 10.5$   $\mu$ m,  $P \ll 0.001$ ). The standard deviation of fiber diameter was not significantly different in the two groups, providing no evidence of fiber degeneration and regeneration in CHO-myostatin muscle.

## REPORTS

g,  $P = 0.015$ ), and retroperitoneal ( $0.012 \pm 0.008$  g versus  $0.033 \pm 0.004$  g,  $P = 0.005$ ) fat pads without affecting intrascapular brown fat [ $0.098 \pm 0.008$  g versus  $0.129 \pm 0.021$  g, *N.S.* (not significant)] (fig. S3; see Materials and Methods in SOM). No reductions in either total body mass or individual muscle masses were observed, however, presumably due to the much smaller amount of myostatin delivered than in the nude mouse experiment.

To explore the mechanism by which myostatin caused muscle wasting, we examined skeletal muscle in non-tumor bearing limbs. Hematoxylin and eosin-stained gastrocnemius sections from wasted CHO-myostatin mice were grossly normal with no evidence of regeneration (Fig. 3A). In particular, we did not observe fibers with greatly varying diameters or centrally placed nuclei. However, morphometric analysis (1) revealed that mean fiber diameter in CHO-myostatin samples was 25% less than in CHO-controls (Fig. 3B), accounting fully for the observed 45% reduction in gastrocnemius muscle mass (Fig. 2C). Myostatin overexpression also caused increased skeletal muscle expression of the cell cycle inhibitor gene, *p21*, and the proapoptotic gene, *bax* (fig. S4; see Materials and Methods in SOM). Taken together, these results support roles for myostatin in regulation of fiber size and cell survival in adult skeletal muscle.

In order to determine whether myostatin induces wasting by causing anorexia, we monitored food intake. CHO-myostatin mice did not consume significantly less food than CHO-controls (Fig. 2I), nor was there gross evidence of malabsorption. Such wasting in the presence of adequate nutritional intake is a hallmark of a condition known as cachexia (17–19). In mice, cachexia can be induced by overexpression of tumor necrosis factor (TNF) (20), interleukin-6 (IL-6) (21), or activin (22, 23), among other factors. TNF and IL-6 serum levels at day 16 were normal in CHO-control or CHO-myostatin mice, however, and neither IL-6 nor TNF

administration resulted in increased skeletal muscle *Mstn* expression (24). Moreover, liver histology was normal in CHO-myostatin mice once weight loss was well established (fig. S5; see Materials and Methods in SOM), in contrast to the hepatic necrosis observed in mice suffering from activin-induced malabsorption and wasting (22, 23). These results are consistent with a role for myostatin in wasting syndromes that is distinct from these other factors.

Lastly, we examined whether systemic myostatin activity could be inhibited by systemic administration of myostatin propeptide or follistatin. CHO-propeptide, CHO-follistatin, or CHO-control cells were injected into the left thigh of athymic nude mice. Twelve days later, CHO-myostatin cells were injected into the other thigh. The presence of CHO-propeptide (Fig. 4A) or CHO-follistatin (Fig. 4B) tumors significantly slowed myostatin-induced weight loss. Thus, systemic administration of myostatin inhibitors can interfere with the activity of myostatin produced at distant sites *in vivo*.

Here we present evidence that myostatin may normally act in an endocrine fashion in adult animals. We have shown that myostatin circulates in a latent form that must be dissociated for biological activity and that systemically administered myostatin can influence muscle and fat mass in adult animals. Thus, myostatin may act as a muscle “chalone,” a term proposed over 30 years ago for a circulating protein that inhibits the growth of a particular tissue and thereby maintains appropriate tissue mass (25, 26). We have also demonstrated that excess myostatin causes wasting in mice, raising the possibility that myostatin may be involved in human cachexia. The cachexia associated with many chronic disease states, including cancer, AIDS (acquired immunodeficiency syndrome), and sepsis, contributes enormously to the morbidity and mortality associated with these diseases (17). The molecular mechanisms underlying cachexia are poorly understood, and no effective therapeutic interventions have

been identified. Additional experiments will be required to determine whether myostatin plays a role in clinical cachexia, because we have not been able to detect human serum myostatin using the assays described in this study. Nevertheless, our demonstration of the systemic inhibitory effects of myostatin binding proteins points to a potential means of interfering with endogenous myostatin activity to enhance muscle mass in a variety of settings, including cachexia.

### References and Notes

1. A. C. McPherron, A. M. Lawler, S. J. Lee, *Nature* **387**, 83 (1997).
2. A. C. McPherron, S. J. Lee, *Proc. Natl. Acad. Sci. U.S.A.* **94**, 12457 (1997).
3. L. Grobet *et al.*, *Nature Genet.* **17**, 71 (1997).
4. R. Kambadur, M. Sharma, T. P. Smith, J. J. Bass, *Genome Res.* **7**, 910 (1997).
5. L. Grobet *et al.*, *Mamm. Genome* **9**, 210 (1998).
6. R. S. Thies *et al.*, *Growth Factors* **18**, 251 (2001).
7. K. Miyazono, U. Hellman, C. Wernstedt, C.-H. Heldin, *J. Biol. Chem.* **263**, 6407 (1988).
8. L. M. Wakefield *et al.*, *Growth Factors* **1**, 203 (1989).
9. L. M. Wakefield, D. M. Smith, K. C. Flinders, M. B. Sporn, *J. Biol. Chem.* **263**, 7646 (1988).
10. P. D. Brown, L. M. Wakefield, A. D. Levinson, M. B. Sporn, *Growth Factors* **3**, 35 (1990).
11. L. E. Gentry, B. W. Nash, *Biochemistry* **29**, 6851 (1990).
12. D. A. Lawrence, R. Pircher, P. Jullien, *Biochem. Biophys. Res. Comm.* **133**, 1026 (1985).
13. S. Schultz-Cherry, J. E. Murphy-Ullrich, *J. Cell. Biol.* **122**, 923 (1993).
14. S. J. Lee, A. C. McPherron, *Proc. Natl. Acad. Sci. U.S.A.* **98**, 9306 (2001).
15. K. Tsuchida *et al.*, *J. Biol. Chem.* **275**, 40788 (2000).
16. T. Zimmers *et al.*, data not shown.
17. M. J. Tisdale, *J. Nutr.* **129**, 243S (1999).
18. M. Grosvenor, L. Bulcavage, R. T. Chlebowski, *Cancer* **63**, 330 (1989).
19. G. Costa, P. Bewley, M. Aragon, J. Siebold, *Cancer Treat. Rep.* **65**, 3 (1981).
20. A. Oliff *et al.*, *Cell* **50**, 555 (1987).
21. K. Black, I. R. Garrett, G. R. Mundy, *Endocrinology* **128**, 2657 (1991).
22. M. M. Matzuk *et al.*, *Proc. Natl. Acad. Sci. U.S.A.* **91**, 8817 (1994).
23. K. A. Coerver *et al.*, *Mol. Endocrinol.* **10**, 534 (1996).
24. T. Zimmers, S.-J. Lee, unpublished observation.
25. W. S. Bullough, *Cancer Res.* **25**, 1683 (1965).
26. ———, *Biol. Rev.* **37**, 307 (1962).
27. N. F. Gonzalez-Cadavid *et al.*, *Proc. Natl. Acad. Sci. U.S.A.* **95**, 14938 (1998).
28. R. Lalani *et al.*, *J. Endocrinol.* **167**, 417 (2000).
29. M. Thomas *et al.*, *J. Biol. Chem.* **275**, 40235 (2000).
30. K. Sakuma, K. Watanabe, M. Sano, I. Uramoto, T. Totsuka, *Biochim. Biophys. Acta* **1497**, 77 (2000).
31. M. Sharma *et al.*, *J. Cell. Physiol.* **180**, 1 (1999).
32. Supported by NIH grants R01HD35887 and R01 CA88866 (to S.-J.L.), by NIH training grant 5 T32 CA09139 (T.A.Z. and L.G.K.), and by funds from Wyeth. Myostatin was licensed by the Johns Hopkins University to MetaMorphix (MMI) and sublicensed to Wyeth. S.-J.L. and A.C.M. are entitled to a share of sales royalty received by the University from sales of this factor. The University, S.-J.L., A.F.E., and A.C.M. also own MMI stock, which is subject to certain restrictions under University policy. S.-J.L. is a paid consultant to MMI. The terms of these arrangements are being managed by the University in accordance with its conflict of interest policies.

### Supporting Online Material

www.sciencemag.org/cgi/content/full/296/5572/1486/DC1  
Materials and Methods  
Figs. S1 to S5  
References and Notes

3 January 2002; accepted 24 April 2002

**Fig. 4.** Inhibition of CHO-myostatin-induced wasting by systemic administration of myostatin propeptide or follistatin. Mice were injected in the left thigh with CHO-control, CHO-propeptide, or CHO-follistatin cells on day 0, then in the right thigh with CHO-myostatin cells on day 12. Shown is the total body weight (days 0 and 12) or tumor-free body weight (endpoint) of mice treated with (A) CHO-control cells (open squares), versus CHO-propeptide cells (solid squares), or (B) CHO-control cells (open circles) versus CHO-follistatin cells (solid circles). \* $P < 0.02$ ; \*\* $P < 0.001$ . Error bars are  $\pm$  SE.  $n = 5$  or 6 mice per point. CHO-control, CHO-follistatin, and CHO-propeptide tumor weights were not significantly different (16).

